heritage

Article

Geophysical Investigations within the Latus Dextrum of Porolissum Fort, Northwestern Romania—The Layout of a Roman Edifice

Alexandru Hegyi [1,2,*], Vlad Lăzărescu [3], Michał Pisz [4,5], László Lenkey [5,6], Mihály Pethe [7], Alexandru Onaca [2] and Mădălina Nica [1]

1 Centre for Southeast Asian Studies, Kyoto University, 46 Shimo-Adachi, Yoshida, Sakyo-Ku, Kyoto 606-8501, Japan
2 Applied Geomorphology and Interdisciplinary Research Centre (CGACI), Department of Geography, West University of Timișoara, 300223 Timișoara, Romania
3 Institute of Archaeology and History of Art of the Romanian Academy, 400085 Cluj-Napoca, Romania
4 School of Archaeological and Forensic Sciences, University of Bradford, Bradford BD7 1DP, UK
5 Faculty of Geology, University of Warsaw, 00-927 Warszawa, Poland
6 Department of Geophysics and Space Science, Eötvös Loránd University, 1053 Budapest, Hungary
7 Hungarian National Museum, Múzeum krt. 14-16, 1088 Budapest, Hungary
* Correspondence: hegyi@cseas.kyoto-u.ac.jp

Abstract: This paper summarizes the results of a recent geophysical investigation carried out at Porolissum, which is considered to be one of the most significant Roman sites in Romania. The geophysical survey was carried out within the latus dextrum of the fort, which is the same location that had been the subject of earlier geophysical surveys as well as older archaeological excavations (1970s) that had uncovered a multiroom building. A cesium vapor total field magnetometer and a multi-electrode resistivity meter for a dense Electrical Resistivity Tomography (ERT) survey were used. Eighty parallel ERT profiles in combination with the emerging total field magnetic data and an antecedent magnetic survey allowed us to complete a more precise interpretation regarding the building that once existed on the left side of Porolissum's Principia (the commander's house). In contrast to the magnetic survey, which only reveals a part of the building's architecture, the ERT survey provides a comprehensive view of the structure's layout. More than 20 rooms could be positively identified, and the existence of further rooms might be deduced from the data. The ERT scan revealed the existence of the building's northern external wall as well, which is not reflected on the magnetic map. Because some parts of the building are not visible on the magnetic map, we can assume that the building was constructed with at least two types of rocks (magmatic and sedimentary). In addition to the archaeological interpretation of the geophysical anomalies, a number of discussions concerning the connection between our survey and the geology of the area were held. The complementarity of the magnetic and resistivity results prompted us to conceive a preliminary 3D reconstruction of the building. Even if the building function is unknown in the absence of reliable archaeological data, it could have been a storage building, a second praetorium, a valetudinarium (hospital), or an armamentarium (weapons storage building). The illustrative reconstruction was completed taking into consideration that the building was a Roman military hospital, which, based on the available data, may be considered a credible assumption.

Keywords: Roman archaeology; Roman fort; Porolissum; Romania; archaeological geophysics; Electrical Resistivity Tomography survey; magnetometer survey

check for updates

Citation: Hegyi, A.; Lăzărescu, V.; Pisz, M.; Lenkey, L.; Pethe, M.; Onaca, A.; Nica, M. Geophysical Investigations within the Latus Dextrum of Porolissum Fort, Northwestern Romania—The Layout of a Roman Edifice. *Heritage* **2023**, *6*, 829–848. https://doi.org/10.3390/heritage6020046

Academic Editors: Raffaele Martorana and Patrizia Capizzi

Received: 29 December 2022
Revised: 16 January 2023
Accepted: 17 January 2023
Published: 19 January 2023

Copyright: © 2023 by the authors. Licensee MDPI, Basel, Switzerland. This article is an open access article distributed under the terms and conditions of the Creative Commons Attribution (CC BY) license (https://creativecommons.org/licenses/by/4.0/).

1. Introduction

The Roman Empire stretched from Scotland in the north to Morocco in the south, and then east along the northern African coast to the Red Sea in the south and the Black Sea in the north (Figure 1A). The European continental sector of the limes followed major

geographical features such as the Rhine and Danube rivers. The regions of Banat and Transylvania in Romania, temporarily incorporated into the Roman Empire as a province of Dacia, were just partly enclosed by the river borders. The Empire's longest section of the terrestrial frontier, with an estimated total length of more than 1650 km, was located in present day Romania [1]. The northwestern area of the former province is the most important and extensively researched in Romania. The site at Moigrad-Porolissum (Sălaj County) (Figure 1B,C) is well-known for its exceptional strategic and military importance as a central part of the complex defensive system of the province. For these reasons, it is considered the best-studied archaeological site in the area [2–5]. Despite the topographically diverse setting of the Roman limes, it should be regarded as a whole, given its primary function of fencing off the Roman world from threats from the outer world.

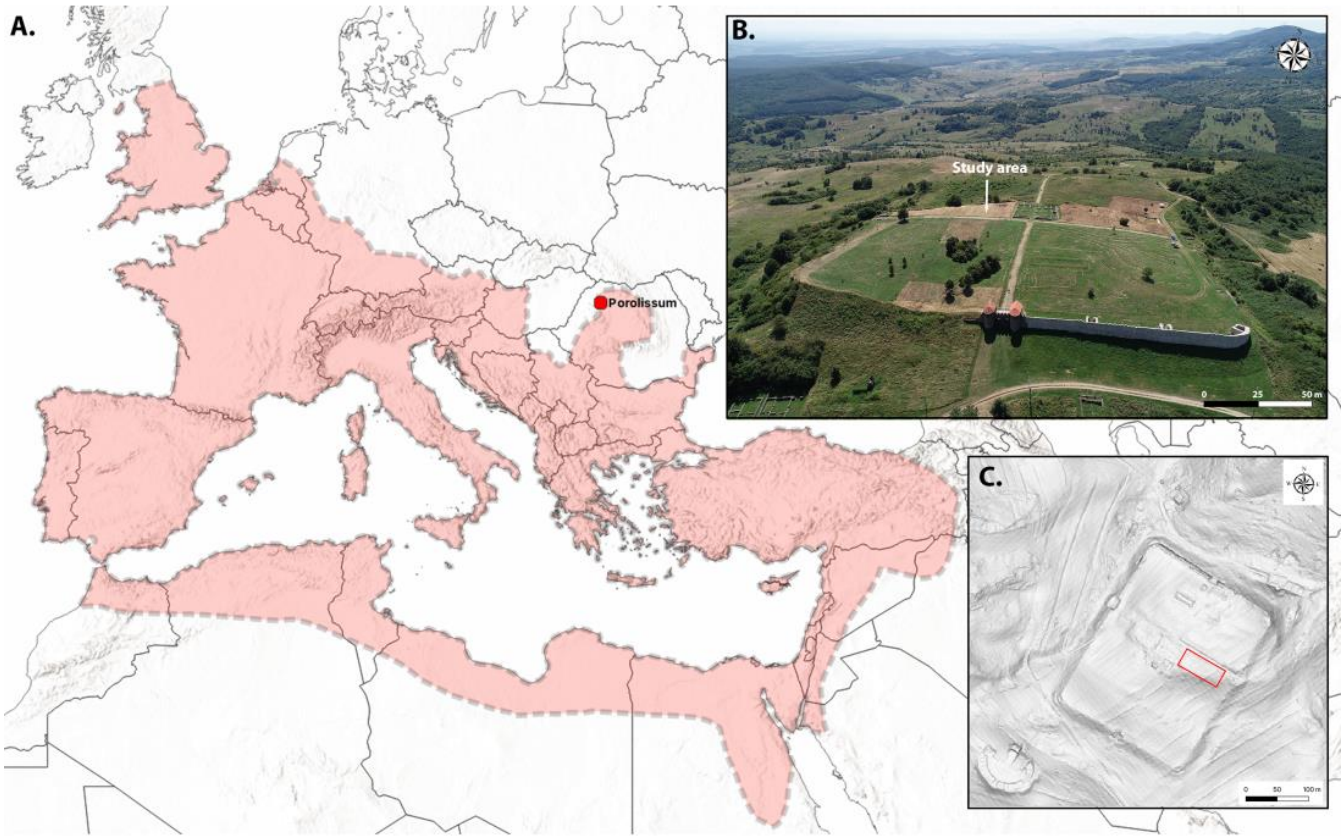


Figure 1. (**A**) Porolissum's location within the Roman Empire's borders; (**B**) Drone view of the Porolissum fort (photo: Ștefan Bilasco, UBB); (**C**) Porolissum's LiDAR digital elevation model. The study area discussed in this paper is depicted in both (**B**,**C**).

The Roman presence tore apart the existing human habitat in the region [6], splitting it with a sophisticated border defense system. Following the region's geography, the whole defense system was built along a series of concentric lines leading into the province's heart, namely the military fort and town of Porolissum. The first defense line consisted of forts manned by infantry auxiliary troops placed in key natural passes. The auxiliary, highly mobile cavalry was positioned behind and able to displace quickly using the road network, while the legions were settled towards the center of the new province. As a result, the limes defense relied on a complex, in-depth system of surveillance, signaling, and communication comprised a network of roads, posts, camps, turf walls, and watchtowers [3,7–10]. Despite the complexity of the defensive system surrounding Porolissum, one should consider the limes more as a "bridgehead" connecting Barbaricum with the Roman world, and not as an impenetrable barrier. Apart from its main military function, the limes also played an

administrative and bureaucratic role, acting as a vector for cultural and economic exchanges on both sides [11,12].

The importance of Porolissum is also highlighted by the fact that during Hadrian's administrative reorganization of Dacia, one of the newly created provinces was named Dacia Porolissensis, making direct reference to the importance of the site [13]. The core of the Porolissum military complex was the fort located at Pomăt Hill, the largest auxiliary Roman fort in the Dacian provinces. Its stone phase was built during the reigns of Hadrian and Antoninus Pius and measured 230 × 300 m (almost three times the typical size of an auxiliary fort) [4]. Despite being systematically excavated since the early 1970s, the inner plan of the fort was revealed only in recent years by means of extensive non-invasive surveys comprising both magnetic and electrical resistivity methods [14,15]. The complexity and the spatial distribution of the components of the defense system surrounding the site were revealed using a LiDAR survey, covering about 14 km^2 [10]. The remote sensing data illustrated the relationship between the above-mentioned auxiliary fort and another, smaller (101 × 66 m), military post located on the neighboring Citera Hill [16]. The military vici that developed around these forts grew constantly until they were transformed into a municipium [9,17]. Beforehand, a series of excavations were performed to establish the extent of the civilian habitation. However, only recent multi-method geophysical surveys were able to establish both the limits and the structure of this settlement [9,15,18–20].

The first geophysical measurements ever taken at Porolissum were performed by Dr. Florin Scurtu in 1996 within the vicus area [21,22]. A Hungarian team led by László Lenkey completed the first geophysical work within the fort in 2008 using a GEM GSM-19 Overhauser Magnetometer in a pseudo-gradient configuration and 1 × 1 m sampling resolution [14,23–25]. In this paper, we will refer to this data as Lenkey's magnetic results or Lenkey's data. Subsequent surveys in 2009–2012, conducted by the same team but with the sampling resolution increased to 0.5 × 0.5 m, covered the entire fortification. The results revealed numerous archaeological structures, facilitating the outline of some important buildings, located within the fort's walls (Figure 2A). One can observe very prominent and self-explanatory magnetic anomalies in the central part of the fort. This area, presumably well-preserved, instantly drew the archaeologists' attention. Further investigations were conducted around the latus sinistrum over the following years (Figure 2B,C). The magnetic measurements were supplemented by Earth Resistance and Electrical Resistivity Tomography (ERT) surveys conducted by Dan Ștefan, a geophysicist and archaeologist (Figure 2B,C). Under Ștefan's supervision, more geophysical measurements were performed outside the fort, in the vicus area. The outcome of this research has been published [9,15,18,19].

The purpose of this study is to present the results of the emerging geophysical survey carried out in the summer of 2020. The measurements were designed to cover an area within the latus dextrum of the fort, where the first magnetic survey revealed an extensive building complex. A more detailed total field magnetic survey was designed for that specific area. To complement the magnetic measurements, we decided to apply high-resolution Electrical Resistivity Tomography (ERT), to create high-definition electrical maps of the subsurface within that area.

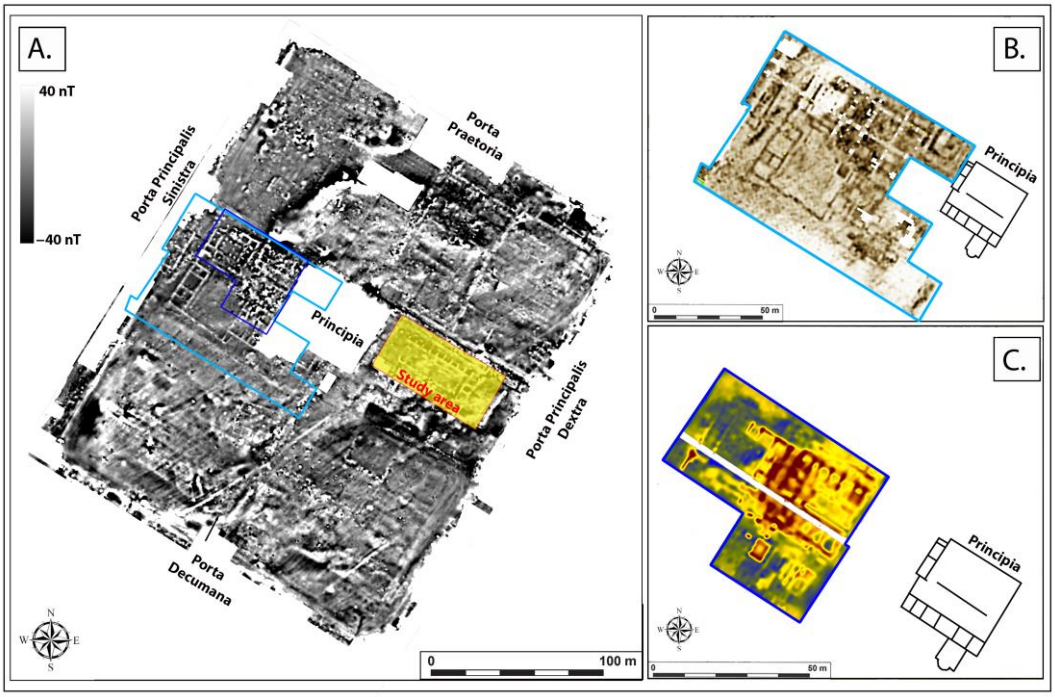


Figure 2. (**A**) Magnetic survey results by László Lenkey and Mihály Pethe—the results were published in various formats in [13,14,20,23]; (**B**) Edited visualization of Earth Resistance Survey within the Latus Sinistrum of the fort conducted by Dan Ștefan published in [14]—Figure 4; (**C**) Edited visualization of a depth slice rendered from the ERT survey data by Dan Ștefan, published in [14]—Figure 5. The spatial extent of surveys shown in (**B**,**C**) is represented with different colors in (**A**). The results were published without a color scale to display the distribution of the values. The study area is depicted in (**A**).

2. Materials and Methods

Based on the results of the previous magnetic gradient survey, we have chosen an interesting structure in the latus dextrum to study further. To capture more details of the structure, we resurveyed it with magnetics (Figure 3A). We used an alkali vapor (cesium) total field magnetometer from Geometrics (G-858) in a duo-sensor configuration. The measurements were made along parallel profiles in 20 × 20 m grids. The traverse interval was 0.5 m, and due to concern for the best outcome data quality, a parallel sampling pattern was selected instead of the zigzag. The sampling rate of the G-858 magnetometer is 10 Hz, which translates roughly to a 0.1 m sample interval at a data collection speed of 1 m/s. Interpolation was used to downsample the data to a 0.125 m sample interval. Dedicated software' were used to process the magnetic data collected. The processing workflow consisted of the use of MagMap [26], MagPick [27], TerraSurveyor [28], and Surfer software [29]. The preprocessing was performed in MagMap, where we aligned the data and removed any undesired stagger. The background was removed in MagPick using a linear function. Further data enhancement employing dedicated filters was performed in TerraSurveyor, and the raster visualizations were rendered in Surfer. ERT was performed with the help of a GeoTom MK8E1000 high-resolution multielectrode system. A total of 80 parallel ERT profiles were measured. The separation between the lines and between the electrodes along the lines was even and equal to 0.7 m. The ERT data were processed and visualized in Res2DInv [30], Res3DInv [31], Voxler [32], and Surfer. The profiles were inverted in Res2DINV using the least squares inversion parameters. The collated file containing all the profiles was inverted in Res3DInv. Voxler and Surfer were used for 2D and 3D visualizations of the processed data. The extracted building footprint allowed us to draw the planimetric morphology of the structure. CAD software was used to deliver

a three-dimensional solid model of the building. To produce the computer-generated imagery (CGI), we used the three-dimensional rendering technique, which is the process of producing an image based on three-dimensional data. The purpose of the reconstructed model was to represent the shape of the building. Less emphasis was placed on the use of realistic textures. The created virtual model should be seen as a simulation, interpretation, and scientific dissemination tool and not as a realistic visual representation.

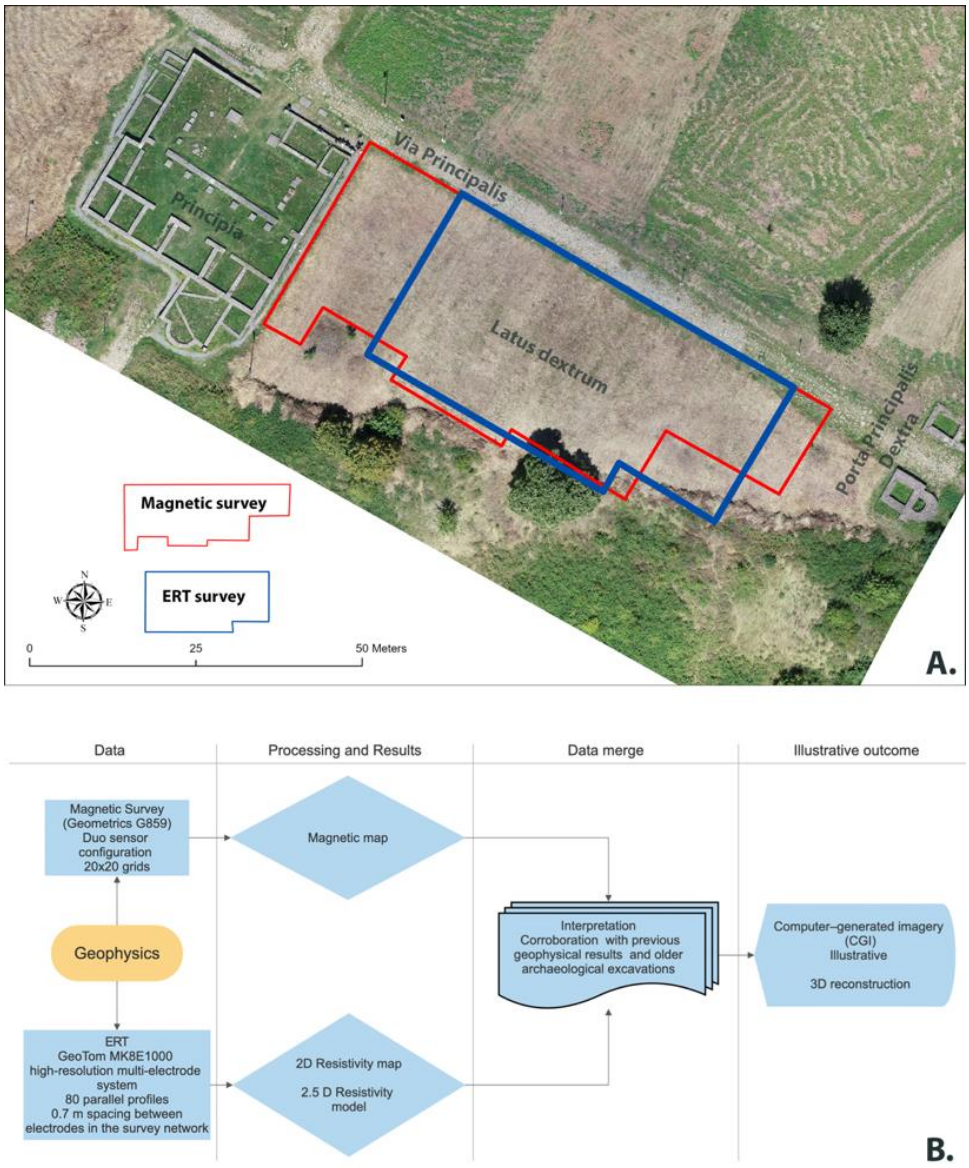


Figure 3. (**A**) The location of 2020's geophysical survey. The red rectangle outlines the area surveyed with a total-field magnetometer. The blue indicates the area where the ERT survey was deployed. The basic methodological workflow used in this paper. (**B**) The methodological workflow used in this paper.

3. Results

According to our estimations, the magnetic survey results (Figure 4) provided a satisfying and slightly more detailed image of the buried structure compared to Lenkey's survey results (see Figure 2A). This is due to a greater sampling resolution (i.e., 0.125 m vs. 0.5 m in Lenkey's survey). The use of a duo-sensor configuration allowed us to plot the magnetic maps of total field values as well. The minimum value recorded was c. 48,860 nT, and the maximum was c. 49,750 nT. The mean value was c. 49,260 nT, the

standard deviation (SD) value was as high as 540 nT, and the magnitude of responses from most archaeological features was in the range of 600 nT. It is noteworthy that these are unusually high values as compared with typical magnetic surveys on other archaeological sites (e.g., the SD value for the gradiometer survey on a Roman fort in Pojejena (Romania) was 11 nT) [33]. In the total magnetic field map, one can clearly discern between local, highly dynamic, and small anomalies and broader, ambient anomalies of smaller amplitudes. Regarding the latter, the most prominent is the diagonal stripe of approximately 15–20 m in width, manifesting as a positive anomaly. Its values oscillate from around c. 49,300 up to c. 49,500 nT in its southernmost part (Figure 5). Outside this anomaly, the recorded background values are around c. 49,150 nT. In addition to background anomalies, a number of linear and zone anomalies of much smaller extent and sharper edges were recorded. The most pronounced are positive linear anomalies, often accompanied by either negative or positive zone or point responses. The measurements with a complementary ERT technique delivered clear and satisfying images of the spatial distribution of substrate-specific electrical resistivity at different depths (Figure 6). The data presented in this paper are discussed in the form of "depth slices," i.e., a series of images compiled by collating all the measured and inverted profiles. The minimum resistivity value recorded was 4.93 Ω.m and the maximum was 2482.46 Ω.m. The average value in the entire dataset is 67.75 Ω.m, while the standard deviation (SD) is 61.08 Ω.m. The inversion RMS error is 5.81%. The ERT results show slightly more elements than the magnetic map. The northern exterior wall of the building represents the most essential element revealed by the ERT data. The precise ERT results also allowed us to better individualize the rooms of the building, as presented in Figure 6A,B.

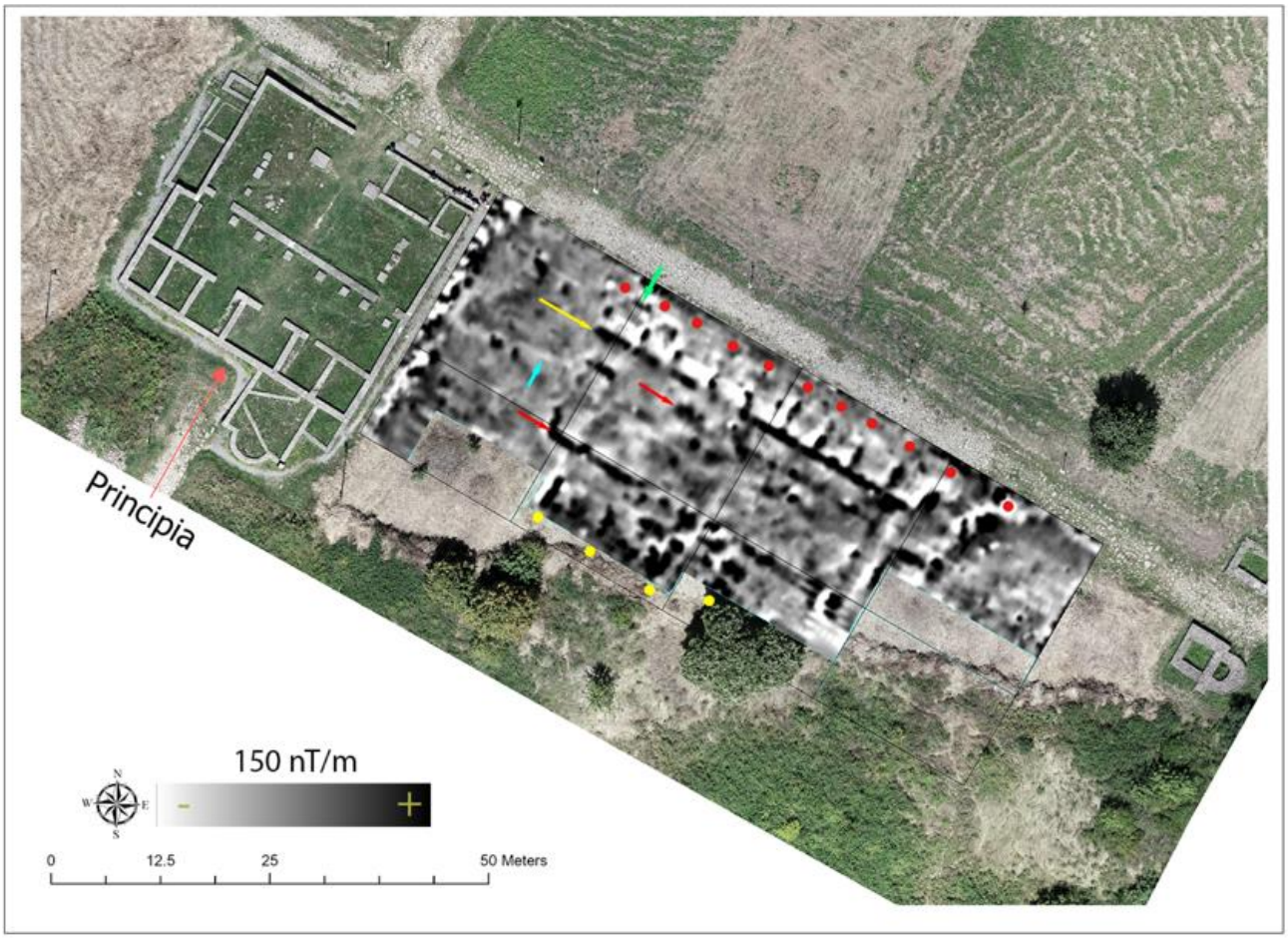


Figure 4. *Cont.*

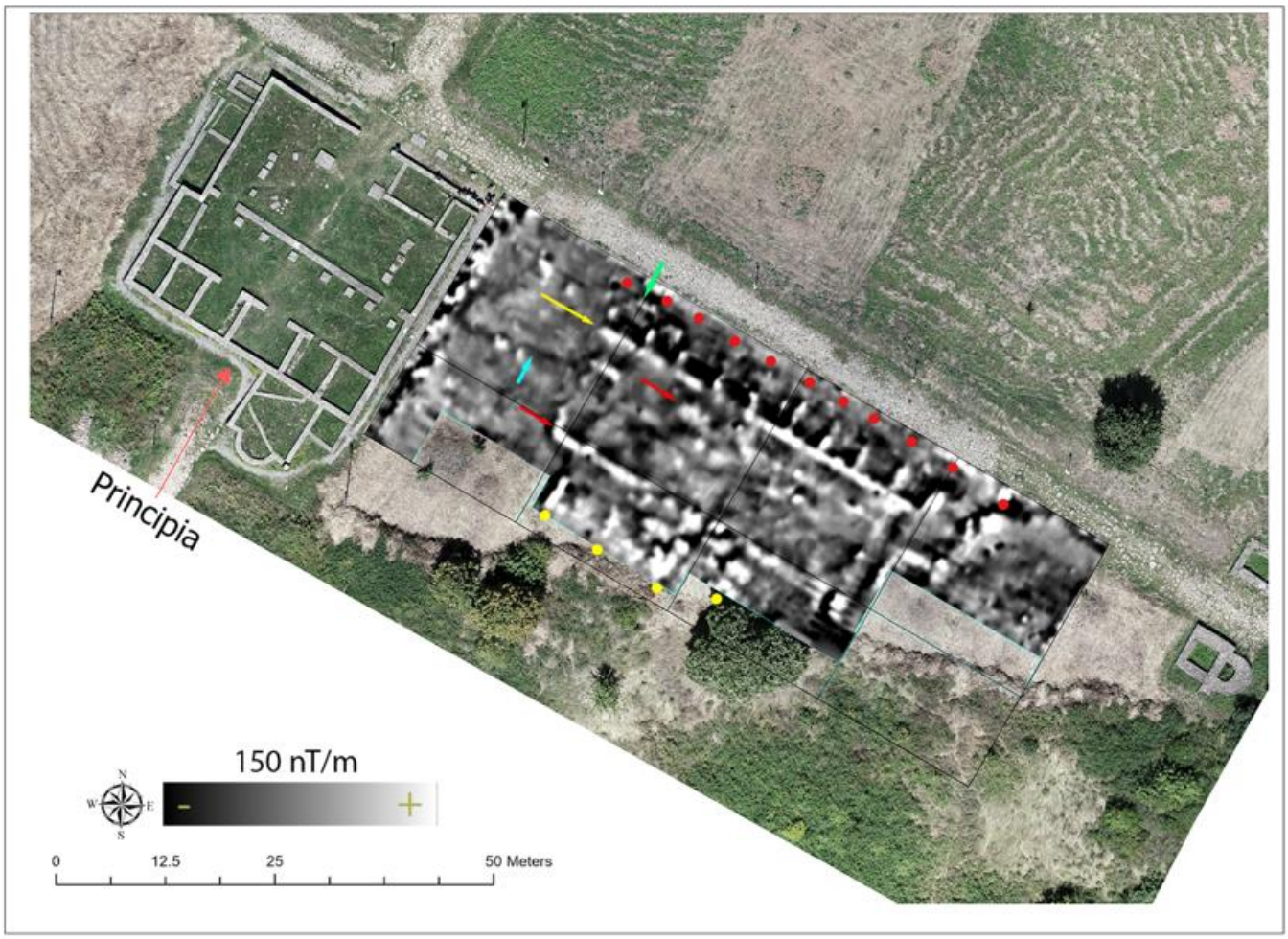


Figure 4. Magnetic survey results were conducted with a Geometrics G859 cesium total field magnetometer in a duo-sensor configuration, with parallel profiles every 0.5 m. The sampling density in 20 by 20 grids is 0.123 × 0.5 m. For both images, the background was removed with a linear function. The top image presents the dynamics of the magnetic value in grayscale, with the negative values being represented by the white color. In contrast, in the bottom image, the values are reversed (the black color represents the negative values). The red and yellow dots mark the ends of small linear anomalies, which are the separating walls of the rooms. The yellow arrow points to one of the longitudinal walls of the building. The green arrow is pointing to the only magnetic anomaly, suggesting the exterior wall of the building. The red arrow indicates other walls, which are most probably the foundation of the courtyard walls. The cyan arrow indicates the location of one of the older archaeological excavations.

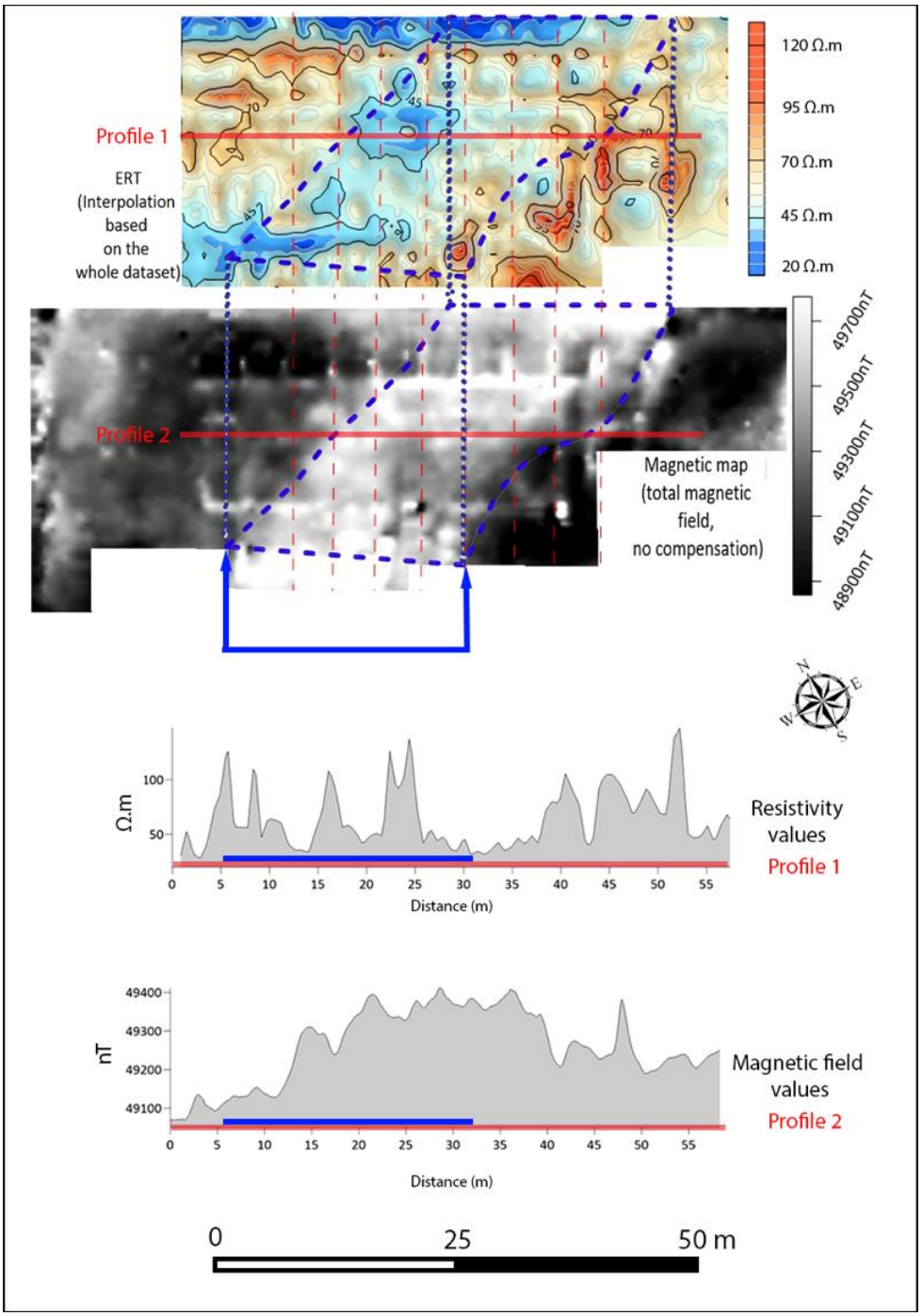


Figure 5. A comparison of magnetic surveys (uncompensated total field) and ERT (interpolation based on the entire dataset). The red lines are used as spatial references. The blue-dotted lines represent the boundary of the local geological formation visible in both surveys. Profiles 1 and 2 depict the local distribution of resistivity and magnetic field values.

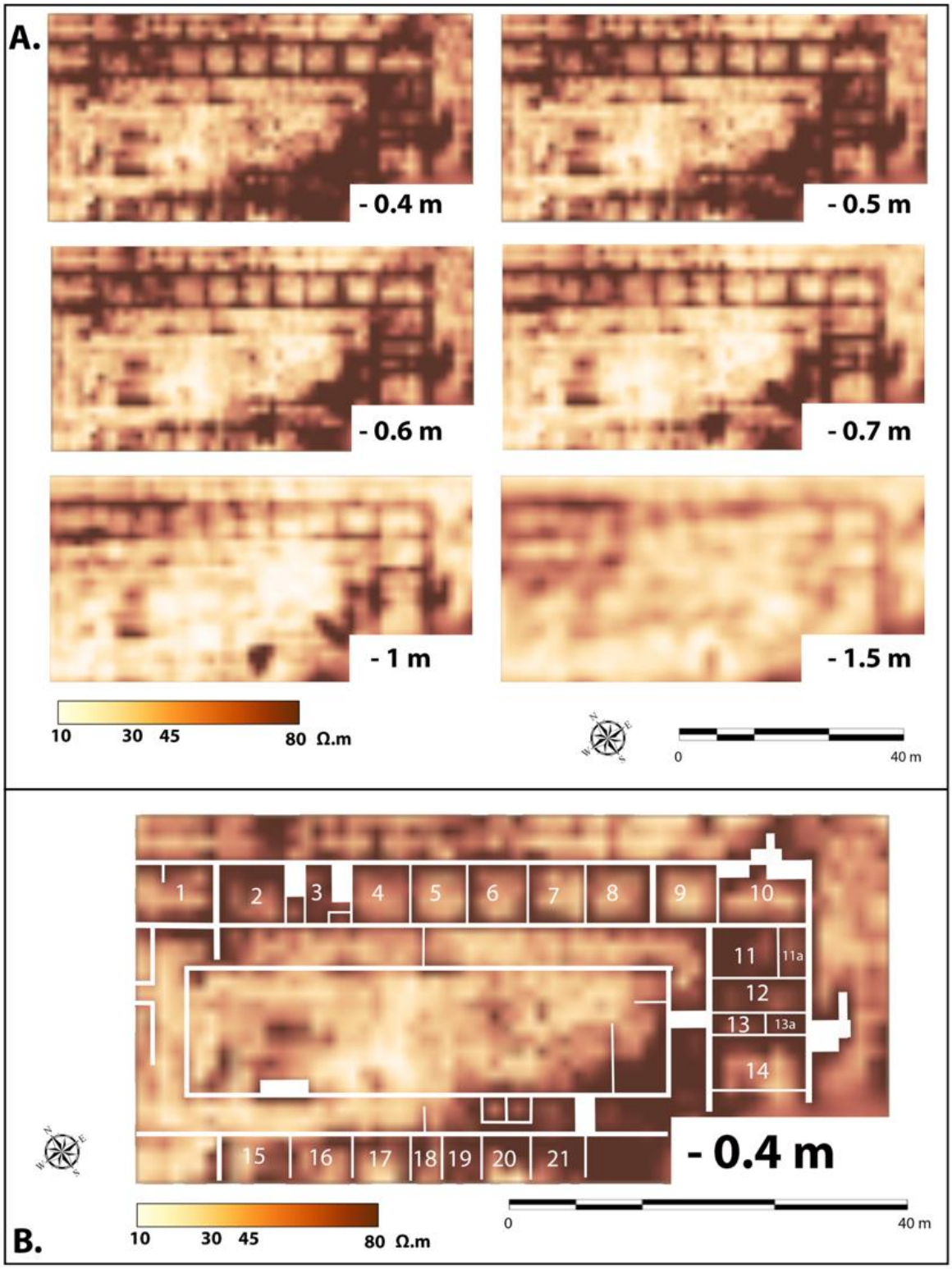


Figure 6. (**A**) Electrical Resistivity Tomography results are presented as subsequent horizontal depth slices. The slices were extracted after the bulk inversion. The drop in the slice's resolution, along with the increment in depth, is an effect of the ERT resolution drop with the increasing depth levels of prospection. (**B**) Interpretation based on the ERT results.

4. Discussions

4.1. Results Interpretation

Both magnetic and ERT survey results delivered clear imagery of buried structures, along with unexpected information on the underlying geology. Furthermore, the results are complementary, i.e., most of the magnetic anomalies coincide with electrical anomalies. On the magnetic map, eleven linear anomalies (marked by red dots at the northern end of Figure 4) can be clearly distinguished in relation to the longitudinal building's walls. These anomalies can be interpreted as walls, running perpendicular to the main north longitudinal anomaly (suggested by the yellow arrow in Figure 4). The emerging magnetometer survey results reveal a succession of rectangular rooms on the building's eastern side. This is the first indication of the existence of an exterior outer wall parallel with the strong lengthwise anomaly marked by the yellow arrow (Figure 4) connecting the 11 smaller linear anomalies. The presence of an exterior wall on the magnetic map is also suggested by a small linear anomaly (Figure 4, green arrow) connecting the first two of the small linear anomalies, and one can see that it is parallel with the main longitudinal anomaly (Figure 4, yellow arrow). The magnetic survey found no other anomalies that pointed to the exterior wall. The existence of the exterior wall was already documented by archaeological excavations conducted by the late professor Nicolae Gudea [3]. The western side of the building is mostly not visible on the magnetic map, except for several anomalies suggesting the building extended slightly more towards the west. The western part was also documented by archaeological excavations (Figure 7A) [3]. Some details of the building's interior are also visible on the magnetic map. For example, another layout, perhaps involving a courtyard or other functional areas, can be seen extending parallel to the strong northern linear anomaly (Figure 4, red arrow). The building's southern half, which rests on the edge of a terrace, appears to be much more intriguing. Unfortunately, erosion has significantly impacted this part of the structure, which may have led to its eventual destruction. The magnetic map shows a succession of anomalies that indicate, most likely, fragments of walls, suggesting that the southern visible linear anomaly (Figure 4) is not the outer wall of the building on that side and that another layout, like the one existing on the northern side, may have existed. Both the older magnetic gradient map and our own, plus the archaeological excavations, provide support for this theory. Regarding the complicated geology in Porolissum and the broad use of highly magnetic rocks as a construction material, one may expect a magnetic survey to deliver well-contrasting anomalies and conclusive results. However, as this paper proves, even in such a setting, additional and complementary methods should be considered and are strongly recommended since they may shed new light on what seem to be clear and conclusive results. The ERT results provided emerging information on how the edifice in the latus dextrum might have looked, and even more, they possibly indicate the existence of an earlier structure underneath. The depth slices, presenting the horizontal distribution of the ground's electrical resistivity, clearly outline the layout of the building. The tops of the linear high-resistant features can be noticed, ranging between 0.2 and 0.4 m below ground level (BGL). As we interpret these prominent linear anomalies, the walls appear at 0.4 m BGL and are traceable up to approximately 2.0 m BGL. They start to fade at 1.5 m BGL. Keeping in mind that the recorded resistivity value is true for a bulk of soil, we consider that the readings from the lowest levels, where walls are still visible, are affected by the presence of these contrasting features in the layers above. Based on the ERT data, the foundations of the building are estimated to be at 1.2–1.5 m BGL (Figure 6). We were able to distinguish a total of fourteen rooms (with two smaller appendices, 11a and 13a in Figure 6B) on the northern and eastern sides of the structure (Figure 6, marked from 1 to 14). Except for the rooms on the western and eastern extremities of the northern wall line, which have slightly larger interior space (c. 22 m^2), all rooms on the north side are the same size (c. 17 m^2). Two types of interior spaces can be found on the edifice's eastern flank. The first type of interior space is represented by rooms measuring 22 m^2 (Figure 6, rooms 11 and 14). The second type, on the other hand, is represented by small and relatively narrow rooms that could have been used

as storage or even as a staircase (Figure 6, room 13). The existence of an upper floor might be considered based on the width of the anomalies (i.e., the foundation walls) on the eastern side. It is nearly double that of the foundation walls on the northern side. That significant width difference might be caused by a certain technological demand, and the second floor of the building could be a possible explanation. We noticed a remarkably interesting and unexpected occurrence around the depths of c. 1.0–1.2 m BGL. Along with the fading of the mesh of highly resistant linear anomalies, a rectangular, highly resistant anomaly becomes increasingly pronounced along with the depth, reaching the top clarity at depths of 1.5–2.0 m BGL (Figures 6 and 8). This unexpected feature might be interpreted as an earlier structure, possibly well-preserved since it was overbuilt with the large building (Figure 8). The existence of an underlying structure is possible, and from a methodological point of view, this interpretation is consistent with all previous results. As a passive technique, the magnetic method can only record the values of the Earth's magnetic field right over the ground surface. The subsurface and surface features and objects disturb the Earth's magnetic field. However, the intensity of the secondary magnetic fields (i.e., induced, or remanent magnetic fields of the searched features), which are disturbing the Earth's magnetic field (and producing these highly desirable and sought-after anomalies), drops with the inverse cube of the distance from their sources. Hence, the magnetic method has a limited, but hard to conclusively define, depth of resolution. Regarding the depths of the features known from the ERT data and the overall high magnetization of all the features (i.e., andesite rocks) and the surrounding soil, we argue that even well-preserved structures present at greater depth might not be clear, or even might be totally beyond the range of detection, even for the sensitive Overhauser and alkali vapor magnetometers. Since the non-destructive methods require verification to prove their results, we suggest that further research on this structure be carried out. Ground-penetrating radar is another non-invasive method that could be applied to this structure, and if invasive techniques (namely, archaeological excavations) were to be conducted in this area, we argue that the northern corner of the surveyed area, where another structure appears under the shallow building, should be targeted with more detailed archaeological work. However, because the soil resistivity is below 50 ohm.m (Figure 5), the radar waves could decay before reaching the desired target depth of 1.5 m, but it is worth considering it for future investigations within this area. The geophysical data provide information not only about the shape but also about the condition of the structures. The southern part of the building suffered from more extensive degradations, as seen on both magnetic and electrical resistivity maps. On the other hand, the ERT data provide stronger evidence for the existence of another series of rooms (Figure 6, rooms 15 to 21). The walls of at least seven rooms can be seen at 0.4 m BGL (Figure 6, rooms 15 to 21). Given the building's symmetry, we can assume that the rooms on the southern side would have followed the same alignment as those on the northern side. Rooms 19, 20, and 21 (Figure 6) might have had a different layout, as differences in their sizes can be observed. Room 19 (Figure 6) might have been a hallway. Other small dependencies can be observed on the southeastern corner of the building toward the interior (Figure 6, red arrows). The central part of the building displays further linear anomalies on both the magnetic and geoelectric maps. Magnetic readings taken from the northeast corner of the building reveal the presence of additional walls within the area bounded by the main foundation. The existence of a rectangular structure within is clarified further by the ERT results (Figure 6, blue arrows). These rectangular foundations are noticeably thinner than those of the main building. A courtyard with various dependencies or an open courtyard could have existed here. It's possible that the columns sustaining part of the roof were built on top of these thinner foundations. To support this idea, we point out the distribution of magnetic anomalies in the building's northeast corner, where the linear anomaly appears broken up by a series of smaller circular anomalies spaced at regular intervals. We realize that only further archaeological excavations can best confirm or deny this theory. We can only indicate the existence of that internal structure at this time. Unfortunately, the space inside this rectangular enclosure cannot be explained by

geophysics at this moment. The area enclosed by the rectangular foundations is roughly 344 square meters. The construction of the building seems to be significantly less complex on the western side. The only features that can be seen in the magnetic data are the foundations of a single wall line, and there is no indication of the presence of any rooms. Unfortunately, the ERT survey area was positioned according to the magnetic map, and as a result, it does not fully cover the desired extent, leaving the results inconclusive. On the other hand, some of the magnetic anomalies may suggest that the building's entrance was located on its western side. The traces of one of professor Gudea's archaeological excavations are represented by the linear negative magnetic anomaly, which runs east–west perpendicular to the building's western wall (Figure 4, cyan arrow).

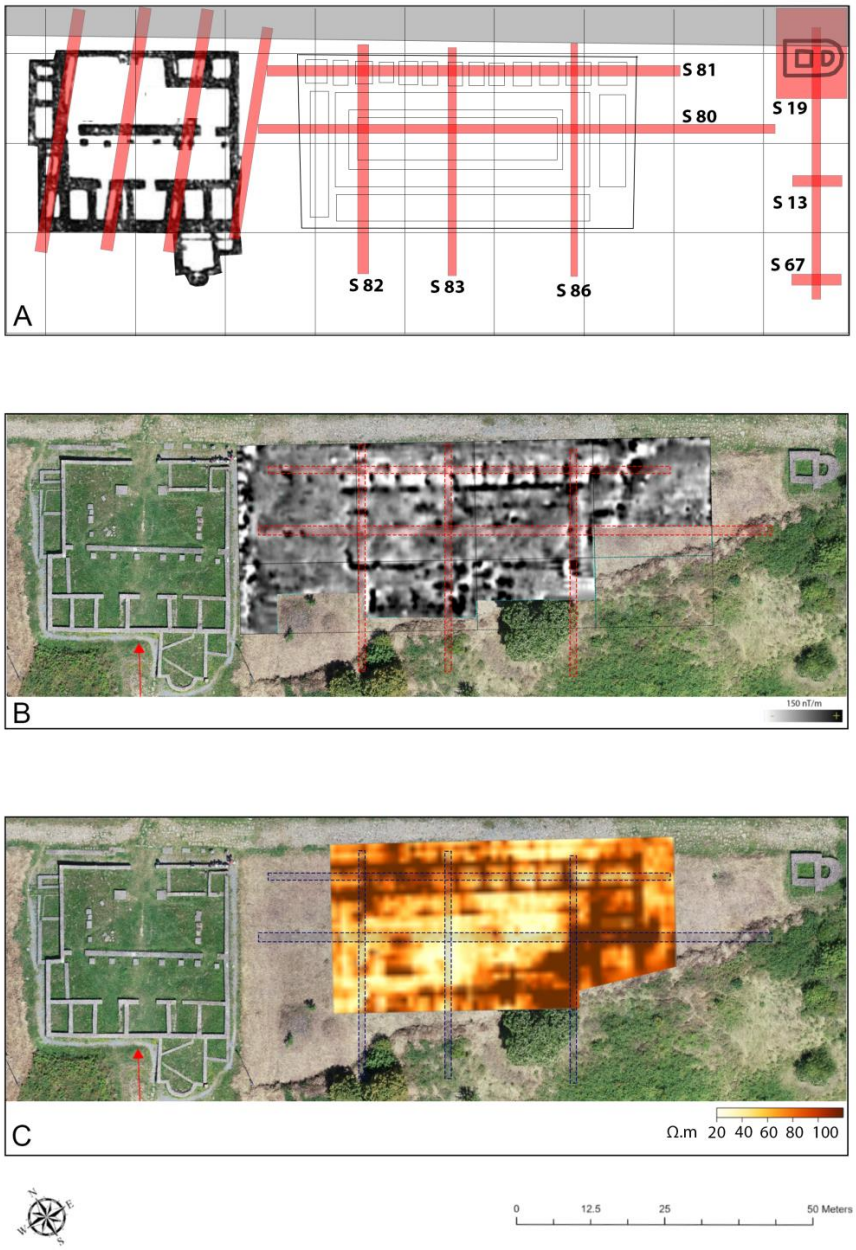


Figure 7. Comparison of old archaeological excavations with the geophysical results. (**A**) Archaeological sections (S80, 81, 82, 83 and 86) crossing the building—the image is a georeferenced drawing after the main map published by professor N. Gudea in 1997, [3] Figure 10; (**B**) A magnetic map overlayed by the archaeological sections (with red); and ERT results overlayed on the archaeological sections (with blue). The red arrow on (**B**,**C**) indicates the Principia.

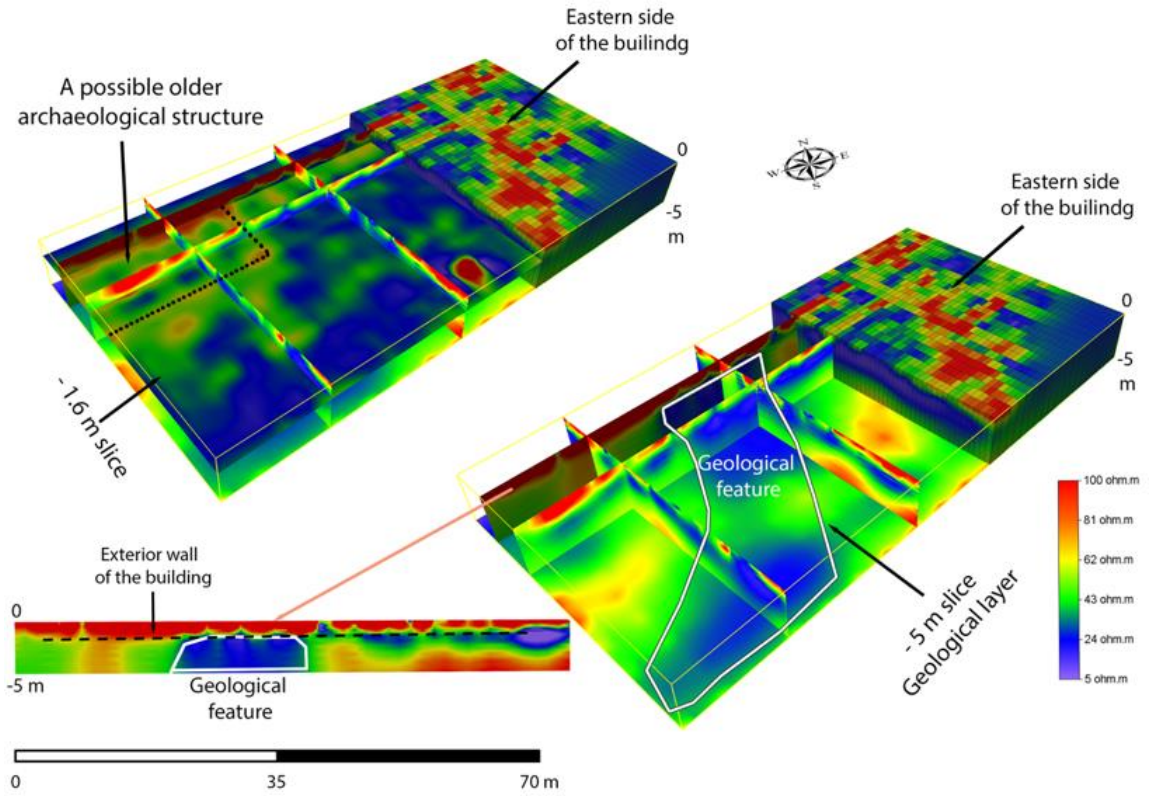


Figure 8. ERT results—a 2.5D visualization. This visualization was used to illustrate the delineation of naturally occurring geological formations up to 5 m BGLBLG (**bottom**) and a possible older archaeological visible at 1.6 BGLBLG (**top**).

4.2. The Impact of the Geological Setting on the Results of Archaeological Prospection

The nature of the geophysical anomalies at the Porolissum site is particularly interesting. Typically, in archaeological prospection, the most visible anomalies to be captured with a magnetic survey are those caused by in situ heating. That induces processes leading to a thermoremanent magnetization of features [34,35]. However, in the fort's latus dextrum, thermoremanent anomalies are not commonly present. The anomalies we interpret as building walls and foundations remain, but they are of a different origin. These are induced magnetic anomalies [34], i.e., derived from the features of considerably high magnetic susceptibility. This can be concluded based on the negative part of the anomalies, visible only in the northern part of each anomaly. The local increase in magnetic susceptibility is the effect of using igneous rocks (andesite) as a construction material for most of the Porolissum edifices. The site is set in a complex geological context [36]. Figure 9 shows that the site is located in the proximity of an andesite dome called Magura Hill (pointed by the western black arrow in Figure 9). Besides the andesite, dacitic volcanic tuff was also used for different purposes. A volcanic tuff quarry is already known to exist within the area [37].

The considerable magnitude of magnetic anomalies from the structures remains due to the use of igneous rocks as a construction material in Porolissum. This occurrence is particularly prominent in the central part of the fort, where one can delineate some buildings, including some distinctive features, e.g., what might be the atrium's column bases (Figure 10). However, in the other parts of the forts, anomalies seem to be vaguer. Structures are less clear, sometimes even hardly distinctive, and have a clearly smaller amplitude. There are a few possible explanations for this occurrence. Firstly, the archaeological structures might have been constructed using materials of lower magnetic susceptibility, even a different kind of rock, that could produce the inverted contrast, i.e., a negative magnetic anomaly. One of these negative anomalies could be observed in Lenkey's data, south of the 2020 study area, and several faint negative anomalies can be spotted in the

fort's retentura (Figure 10). Some prominent magnetic anomalies that could be spotted in this dataset represent the underlying geology. Another interesting phenomenon can be observed in both Lenkey's and 2020's datasets. This is a fine example of the mutual dependencies between the site's geology and archaeological features. In the recent magnetometer survey data, a local enhancement of the strength of anomalies related to that part of the structure can be noticed. This is better visualized in the non-compensated total magnetic field data plot (Figure 5). We claim that this local enhancement is related to the geological background. This geological formation can be noticed in Lenkey's gradiometer data as well (Figure 10, between the red lines). It is less pronounced in this dataset, as the pseudo-gradient configuration of the measurement is meant to remove the unwanted regional magnetic field variations, attributed to the local geology, and emphasize local, small-scale changes, attributed to archaeological features. We argue that the interpretation of this subtle information delivered in both magnetic datasets is that the local geological formation, made of highly magnetically susceptible material, might bear some residual magnetization as well. The local geological formation's strong magnetic field increases the value of the ambient Earth's magnetic field. That leads to an increase in the value of the magnetic field induced in the archaeological feature and explains why a part of the walls produces a stronger magnetic anomaly than the rest.

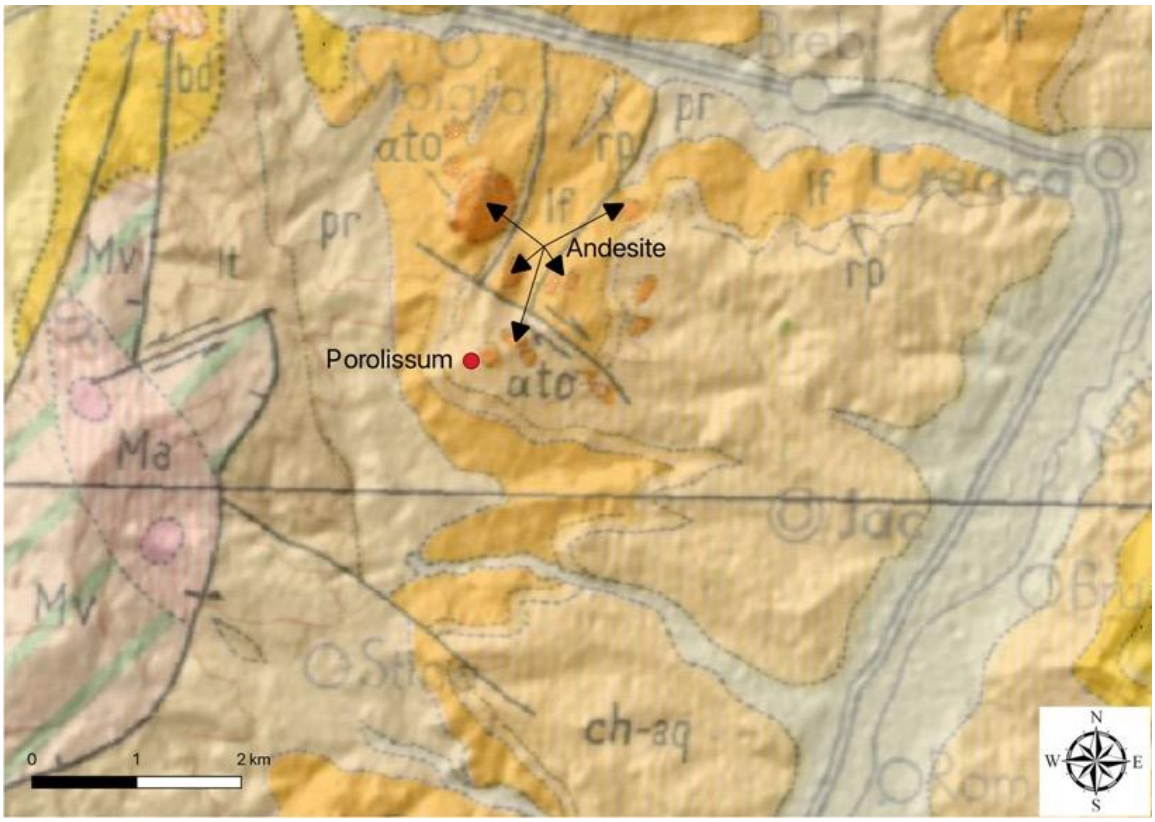


Figure 9. Geological Map of Romania, scale 1:200,000, extract from L-34-XII sheet, Geological Institute of Romania. Map source: https://geoportal.igr.ro/viewservices (accessed on 20 December 2022). Black arrows point to the mapped andesite bodies.

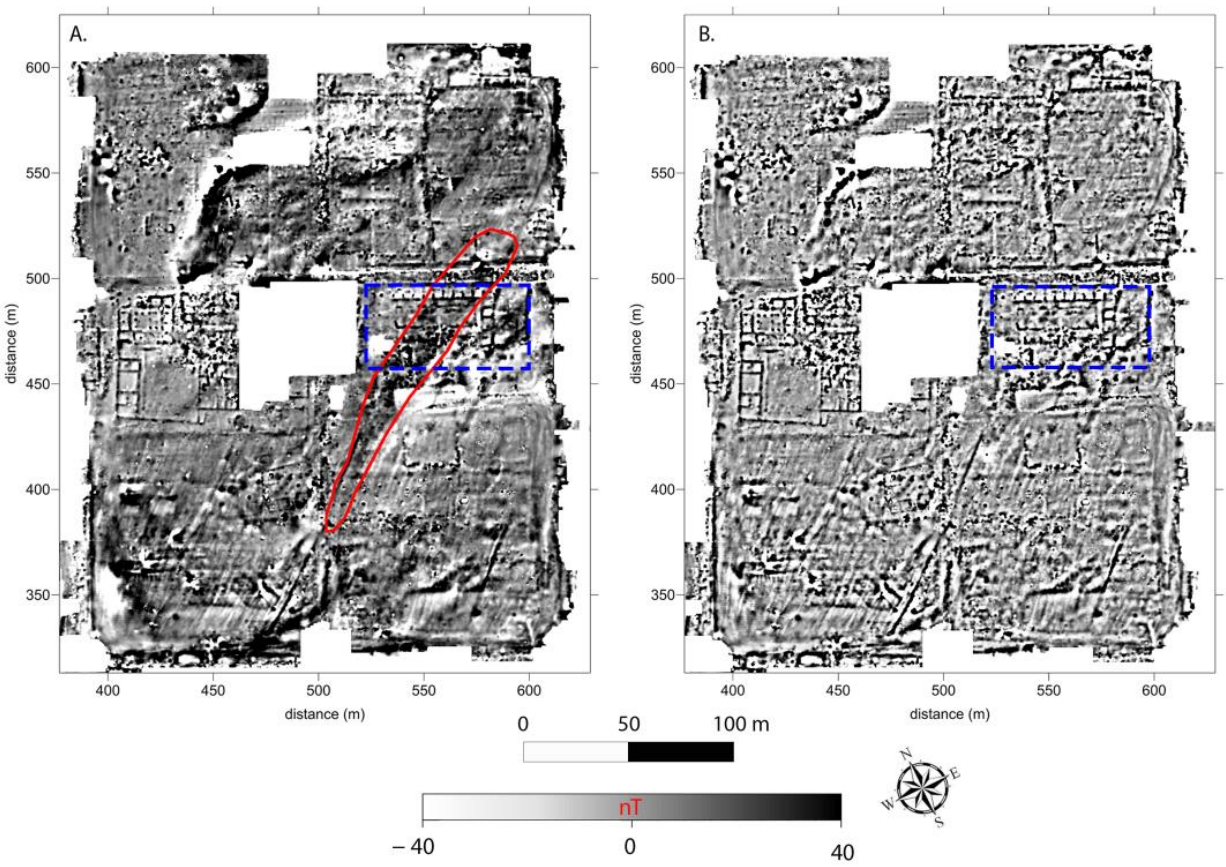


Figure 10. The magnetic survey at Porolissum conducted by László Lenkey and Mihály Pethe. Results were published in various formats in [14,23,24]. (**A**) Magnetic map—basic filtration; (**B**) Filtered magnetic map—geological background removed. The area represented by the red polygon on (**A**) represents a stripe of local geological formation.

A vestige of the tertiary field can be seen in Figure 5, especially in the non-compensated total field magnetic maps. The removal of background geology also decreased the magnetic trace of the local geological formations. The existence of the prominent local geological formations is also visible in the electrical data (Figure 5). The comparison shown in Figure 5 delineates the local geological formation on both magnetic and electrical maps. A single profile trace plot on both magnetic and electrical maps shows that the absolute magnetic field values match relatively low resistivity values to a significant extent. The low resistivity values develop with depth and describe the shape of the local geological formation between 1 and 2.5 m deep (Figures 5 and 8). The geological formation appears on the magnetic map as a positive magnetic anomaly. At the same time, the material tends to be of rather low resistivity (~10–100 Ω.m); hence, the resulting electrical anomaly is described by low resistivity on the ERT composite map. The existence of clays with higher magnetic susceptibility is most likely described by high magnetic anomaly coupled with low resistivity. The existence of red clay with higher magnetic susceptibility was archaeologically documented in the past within the site necropolis.

4.3. An Attempt at Building Reconstruction Based on the Geophysical Results and Older Archaeological Excavations

The complementarity of both datasets provided information of great archaeological value. The results shed new light on the interpretation of the building's layout, mostly by proving the existence of an exterior wall on the northern side. The northeastern closure wall is present in the ERT data (Figures 6 and 7C) and in the archaeological excavations (Figure 7A). Still, it is barely visible on the magnetic maps (Figures 4 and 7B), as is the west-

ern part of the building. There is one explanation for this, based on the joint interpretation of magnetic and electric data: most of the building was built of andesite, except for its northeastern wall and the western side of the building, which were constructed of different building materials, probably limestone. This may be because this wall faced via Principalis, and the western side of the building was facing Principia. Because it is white, in contrast to the ubiquitous darker andesites, limestone would be more decorative. To support this hypothesis, it is worth noting that the use of limestone in Porolissum has already been reported [38]. The only peculiarity might be the lack of a negative linear anomaly visible in the magnetic data. The older general studies about Porolissum depict the building, based only on the former magnetic survey, as having one more extension to the east [14,23,24]. Considering the present results, mainly the ERT, we have no reason to believe that the building had another extended module to the east. The existence of a parallel wall on the eastern side about 10 m away (Figure 10) could indicate the presence of another building or an exterior courtyard. Of course, the extension of the geoelectrical survey within that area could explain this situation better. The extension of ERT or any other active geophysical measurements to the west up to the Principia's eastern wall would clarify the layout of the building even more precisely and would reveal if other rooms or the entrance are located on that side. The discussed building used to be interpreted in many ways, with distinct functions being attributed to it. Initially, due to its plan and analogies with other similar buildings uncovered in the province of Dacia, it was considered a praetorium (commander's building). Still, other functions have also been proposed, such as the valetudinarium or armamentarium. The access from the long side of the building would have led to an inner courtyard with a portico [3,4]. However, the limited archaeological material discovered so far makes this interpretation relatively difficult to sustain [39]. Recent studies have advanced with great probability the hypothesis that the praetorium was situated in the latus sinistrum [15], making the use of this building uncertain. While a second praetorium is still possible (due to the large number of troops stationed at Porolissum [40], it is also possible that it served as a warehouse or storage space based on its planimetry and the archaeological material discovered [41]. To better understand the geophysical data, we produced an illustrative model reconstruction of how the building might have looked. The decisions on the reconstruction on which the virtual model is based were guided by information from geophysical surveys (Figure 7B,C), older archaeological excavations (Figure 7A), historical material, and technical and typological aspects considering comparisons with similar structures and buildings. The traces of the underground structure, discovered by magnetic and electric surveys, were merged to reproduce the configuration of the building (Figure 7). Having no definite physical evidence to show us a concrete volume, the reconstruction of the building can be an ideal three-dimensional architectural visualization or model, based on comparisons with similar structures discovered over time. The reconstruction was made considering the scenario that the building was used as a storage building or as a Roman hospital (valetudinarium), which, based on the building planimetry, is not that improbable.

The first step in the reconstruction process was obtaining a two-dimensional planimetric image based on the corroboration of all existing data. The older archaeological excavations were corroborated with the geophysical results after a preliminary georeferencing of the main map published by Professor Gudea in 1997 [3]. With no detailed archaeological evidence, we suppose the general appearance of the building is based on some similar structures at Porolissum and the building contour resulting from the geophysical survey. Considering the standard structure of a Roman military hospital with multiple individual rooms connected in between by a corridor and some other bigger rooms on the eastern side, combined with evidence regarding the existence of a courtyard and the considerable thickness of the walls on the eastern side of the building, which might have housed a two-level structure, we produced two visualizations which can be seen in Figure 11. Figure 11A shows the hypothetical shape of the building with a tile roof, while Figure 11B shows a cutaway view showing individual interior rooms. For the reader to

better understand the landscape and the location of the building within the fort, we have overlaid the 3D-generated model on a panoramic drone photo. The result can be seen in Figure 12.

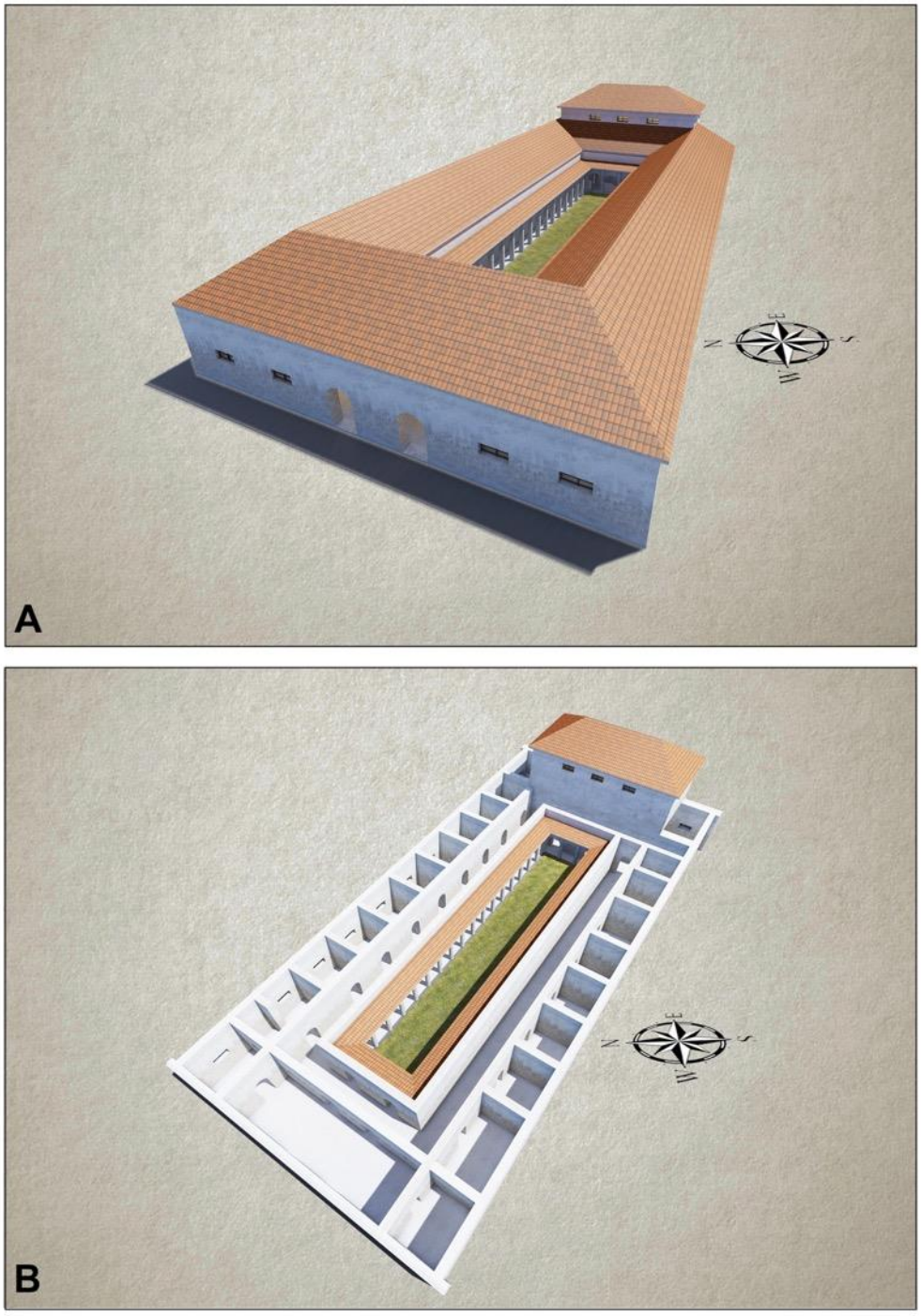


Figure 11. Reconstruction based on geophysical results. (**A**) A broad view of the generated 3D model; (**B**) The same building but with the roof removed to highlight the location of each room, reconstructed from the combined results of the geophysical survey.



Figure 12. Reconstruction based on geophysical results. An oblique drone image (courtesy of Ștefan Bilaşco, UBB) was overlaid and blended with the generated 3D model.

5. Conclusions

The geophysical results presented in this paper shed new light on the archaeological structure of Porolissum fort's latus dextrum. The combination of passive and active geophysical methods was effective in highlighting various elements of the building in the in Porolissum, as the combined used of geophysical methods was proven efficient in other archaeological sites from central and western Romania [21,22,33,42–49]. If the magnetic survey only reveals a portion of the building, the ERT survey provides a more detailed picture of the structure's layout. Furthermore, the ERT survey clearly defines the building's exterior northern wall, which is not visible on the magnetic map. This implies the use of at least two construction materials within this section of the fort: (1) magmatic rocks traced nicely by the magnetic survey, and (2) sedimentary rock (most likely limestone) with weak magnetic properties detected only by the ERT survey. The sedimentary rock (limestone) was most likely used for decorative purposes on the exterior wall facing the Via Principals. The building's internal layout was also revealed. A 3D reconstruction of the building was created using corroborating archaeological and geophysical data. The reconstruction was virtually integrated into the site's landscape for a better understanding of the building's characteristics. Our geophysical survey revealed information about the local geology in addition to archaeology, which is extremely important for planning future geophysical work.

Author Contributions: Conceptualization, A.H.; Data curation, A.H., L.L. and M.P. (Mihály Pethe); Investigation, A.H., V.L., L.L. and M.P. (Mihály Pethe); Methodology, A.H. and M.P. (Michał Pisz); Project administration, A.H.; Resources, A.H. and A.O.; Software, A.H.; Supervision, A.H.; Visualization, L.L., M.P. (Mihály Pethe) and M.N.; Writing—original draft, A.H. and V.L.; Writing—review & editing, A.H., V.L., M.P. (Michał Pisz), L.L., M.P. (Mihály Pethe), A.O. and M.N. All authors have read and agreed to the published version of the manuscript.

Funding: This research received no external funding.

Institutional Review Board Statement: Not applicable.

Informed Consent Statement: Not applicable.

Data Availability Statement: Not applicable.

Acknowledgments: We would also like to thank: Sergiu Socaciu, Vlad Bologa, Denisa Grosu, Teodor Talos and Hanna Meda Ionescu for their help in the field.

Conflicts of Interest: The authors declare no conflict of interest.

References

1. Teodor, E. *The Invisible Giant: Limes Transalutanus. An Overview South of Argeş River*; Editura Cetatea de Scaun: Târgoviște, Romania, 2015.
2. Gudea, N. *Porolissum, un Complex Daco-Roman la Marginea de Nord a Imperiului Roman, Cercetări şi Descoperiri Arheologice pînă în anul 1977: Acta Musei Porolissensis*; Muzeul National de Istorie a Transilvaniei: Cluj-Napoca, Romania, 1989.
3. Gudea, N. *Der Meseş-Limes. Die Vorgeschobene Kleinfestungslinie auf den Westlichen Abschnitt der Grenze der Provinz Dacia Porolissensis/Limesul de pe Munţii Meseş. Linia înaintată de Turnuri de pază de pe Sectorul de vest al Provinciei Dacia Porolissensis*; Zalău, Editura Muzeului Județean de Istorie și Arheologie Zalău: Zalău, Romania, 1997.
4. Gudea, N.; Papp, E. Das Römergrenzkastell von Moigrad- Pomet. Porolissum 1. In *Ghid al Monumentelor Arheologice Din Dacia Porolissensis*; Muzeul Județean de Istorie și Artă Zalău: Zalău, Romania, 1997.
5. Tamba, D.G. *Porolissum: Aşezarea civilă (vicus Militaris) a Castrului Mare*; Editura Mega: Cluj-Napoca, Romania, 2008.
6. Pop, H. *Fortificațiile Dacice din Vestul și nord-Vestul României*; Editura Mega: Cluj-Napoca, Romania, 2006.
7. Gudea, N. The Defensive System of Roman Dacia. In *Britannia*; Society for the Promotion of Roman Studies: London, UK, 1979; Volume 10. [CrossRef]
8. Gudea, N.; Gudea, A.I.; Salontai, S.; Lisovschi-Cheleșanu, C. *Porolissum: Un Complex Daco-Roman la Marginea de Nord a Imperiului Roman. II, Vama Romană: Monografie Arheologică. Contribuţii la Cunoaşterea Sistemului Vamal din Provinciile Dacice*; Muzeul Național de Istorie a Transilvaniei: Cluj-Napoca, Romania, 1996.
9. Opreanu, C.H.; Lăzărescu, V.A. The evolution of the civilian settlement at Porolissum in the light of the new research. *Ephemer. Napoc.* **2016**, *26*, 107–120.
10. Roman, A.; Ursu, T.M.; Fărcaş, S.; Opreanu, C.H.; Lăzărescu, V.A. Documenting ancient anthropogenic signatures by remotely sensing the current vegetation spectral and 3D patterns: A case study at Roman Porolissum archaeological site (Romania). *Quat. Int.* **2019**, *523*, 89–100. [CrossRef]
11. Whittaker, C.R. *Frontiers of the Roman Empire: A Social and Economic Study*; Johns Hopkins University Press: Baltimore, MD, USA, 1994.
12. Opreanu, C.H.; Lăzărescu, V.A.; Ardevan, R.; Găzdac, C.R.; Gui, m.; Ionescu, C.; Pop, H.; Pripon, E.; Simon, V. *A Roman Frontier Marketplace at Porolissum in the Light of Numismatic Evidence, Contribution to the Knowledge of the Roman Limes Economy*; Editura Mega: Cluj-Napoca, Romania, 2015.
13. Russu, I.I. *Inscriptiile Daciei Romane, Volumen 1, Introducere Istorica si Epigrafica, Diplomele Militare, Tablitele Cerate*; Academiei Republicii Socialiste Romania: Bucureşti, Romania, 1975.
14. Fiedler, M.; Höpken, K.; Pánczél, S.P.; Bajusz, I.; Döhner, G.; Lenkey, G.; Merzenich, C.; Pethe, M.; Vasáros, Z. *Porolissum. Forschungen im Kastell auf dem Pomet von 2009 bis 2011*; Müller, K., Schiller, B., Der Fachschaftsrat Des Winckelmann-Instituts Der Humboldt–Universität Zu Berlin , Eds.; Logos: Berlin, Germany, 2011; pp. 449–468.
15. Opreanu, C.H.; Lăzărescu, V.A. The roman headquarters on the northern limes of dacia: Porolissum (jud. sălaj/ro) in the light of recent research. *Archaol. Korresp.* **2020**, *50*, 225–240.
16. Opreanu, C.H.; Lăzărescu, V.A. New light on a Roman fort based on a Lidar survey in the forested landscape from Porolissum. *Ephemer. Napoc.* **2014**, *24*, 71–86.
17. Ardevan, R. *Viaţa Municipală în Dacia Romană*; Mirton: Timişoara, Romania, 1998.
18. Opreanu, C.H.; Lăzărescu, V.-A.; Ștefan, D. Noi cercetări la Porolissum. *Analele Banatului* **2013**, *21*, 83–106.
19. Opreanu, C.H.; Lăzărescu, V.A. *Landscape Archaeology on the Northern Frontier of the Roman Empire at Porolissum*; An Interdisciplinary Research Project; Mega: Cluj-Napoca, Romania, 2016.

20. Opreanu, C.; Lăzărescu, V. The basilica of the forum at Municipium Septimium Porolissense (Dacia). In *Visy 75 Artificem Commendat Opus*; Studes in Honorem Zsolt Visy; Farkas, G.I., Nemeny, R., Szabo, M., Eds.; CLIR Research Center: Pécs, Hungary, 2019; pp. 396–415.
21. Scurtu, F. Radiografia geofizică a unei părţi a oraşului roman Porolissum. *SCIVA* **1997**, *48*, 361–372.
22. Scurtu, F. The geophysical image of a part of the ancient Roman town Porolissum in Dacia. *BAR Int. Ser* **2002**, *1043*, 165–169.
23. Petrovszki, J.; Lipovics, T.; Lenkey, L.; Pethe, M.; Ferencz, E.; Herein, M. Régészeti kutatás céljából végzett mágneses mérések Porolissumon. *Magyar Geofizika* **2008**, *49*, 88–95.
24. Lipovics, T.; Lenkey, L.; Pethe, M.; Herein, M.; Ferencz, E.; Bajusz, I. Masuratori arheomagnetice la Porolissum. *Acta Musei Porolissensis* **2008**, *30*, 123–133.
25. Pethe, M.; Lenkey, L. Magnetic Surveying in the Roman Age Fort of Porolissum. In Proceedings of the 6th Congress of the Balkan Geophysical Society, European Association of Geoscientists & Engineers, Budapest, Hungary, 3–6 October 2011; p. 262.
26. Geometrics Inc. *Magmap 2000 User Guide*; 24891-01 Rev. H; Geometrics Inc.: San Jose, CA, USA, 2000.
27. Tchernychev, M. MAGPICK-Magnetic Map & Profile Processing, User Guide. 2013. Available online: Http://Sourceforge.Net/Projects/Magpick (accessed on 20 December 2022).
28. Terra Surveyor, User Manual, Program Verion 3.0. Available online: https://dwconsulting.nl/Download/TerraSurveyor%20manual%203033.pdf (accessed on 20 December 2022).
29. Surfer® from Golden Software, LLC or Surfer® (Golden Software, LLC), Golden Software, LLC, PO Box 281, Golden, CO 80402-0281 USA. Available online: www.goldensoftware.com (accessed on 20 December 2022).
30. Loke, M.H. *Rapid 2-D Resistivity and IP Inversion Using the Least-Squares Method*, Geoelectrical Imaging 2D and 3D Geotomo Software; Geotomo Software: Penang, Malaysia, 2002.
31. Loke, M.H. *Res2Dinv and Res3dinv Software, Version 3.59, Geoelectrical Imaging 2D&3D*; Geotomo Software: Penang, Malaysia, 2009.
32. Voxler® from Golden Software, LLC or Voxler® (Golden Software, LLC), Golden Software, Golden, CO, USA. Available online: www.goldensoftware.com (accessed on 20 December 2022).
33. Pisz, M.; Tomas, A.; Hegyi, A. Non-destructive research in the surroundings of the Roman Fort Tibiscum (today Romania). *Archaeol. Prospect.* **2020**, *27*, 219–238. [CrossRef]
34. Fassbinder, J.W.E. Seeing beneath the farmland, steppe, and desert soil: Magnetic prospecting and soil magnetism. *J. Archaeol. Sci.* **2015**, *56*, 85–95. [CrossRef]
35. Fassbinder, J.W.E.; Stanjek, H. Magnetic properties of biogenic soil greigite (Fe3S4). *Geophys. Res. Lett.* **1994**, *21*, 2349–2352. [CrossRef]
36. Seghedi, I.; Ntaflos, T.; Pécskay, Z.; Panaiotu, C.; Mirea, V.; Downes, H. Miocene extension and magma generation in the Apuseni Mts. (western Romania): A review. *Int. Geol. Rev.* **2022**, *64*, 1885–1911. [CrossRef]
37. Wollmann, V. Cercetări privind carierele de piatră din Dacia romană. *Sargetia* **1973**, *X*, 105–122.
38. Zăgreanu, R. Votive Statue Bases and Votive Altars from Porolissum. *Acta Mus. Napocensis* **2016**, *53*, 203–248.
39. Marcu, F. *The Internal Planning of Roman Forts of Dacia*; Mega Publishing House: Cluj-Napoca, Romania, 2009.
40. Opreanu, C.H. The Garrison of the Roman Fort at Porolissum (Dacia). The Analysis of the Tile-Stamps. *Open Archaeol.* **2018**, *4*, 365–372. [CrossRef]
41. Groh, S. *Im Spannungsfeld von Macht und Strategie: Die legio II Italica und Ihre Castra von Locica (Slowenien), Lauriacum/Enns und Albing (Österreich)*; Gesellschaft fuör Landeskunde und Denkmalpflege Oberoösterreich: Linz, Austria, 2018.
42. Hegyi, A. Aplicarea Metodelor Specifice Geoștiințelor in Cercetări Arheologice din Sud-Vestul României. Ph.D. Thesis, Universitatea de Vest din Timișoara, Timișoara, Romania, 2018.
43. Hegyi, A.; Sarris, A.; Curta, F.; Floca, C.; Fortiu, S.; Urdea, P.; Onaca, A.; Timofte, F.; Pisz, M.; Timut, S.; et al. Deserted medieval village reconstruction using applied geosciences. *Remote Sens.* **2020**, *12*, 1975. [CrossRef]
44. Hegyi, A.; Urdea, P.; Floca, C.; Ardelean, A.; Onaca, A. Mapping the subsurface structures of a lost medieval village in South-Western Romania by combining conventional geophysical methods. *Archaeol. Prospect.* **2019**, *26*, 21–32. [CrossRef]
45. Țentea, O.; Matei-Popescu, F.; Călina, V. Frontiera romană din Dacia Inferior. O trecere în revistă și o actualizare. 1. *Cercet. Arheol.* **2021**, *28*, 9–90. [CrossRef]
46. Stavilă, A.; Hegyi, A.; Craiovan, B. Non-invasive archaeological research performed in the Middle Bronze Age settlement from AlioșValea Alioşu (Timiș County, Romania). Structures, chronology, and perspectives. Ziridava Stud. *Arcaheologica* **2020**, *34*, 168–188.
47. Asăndulesei, A. *GIS, Fotogrametrie și Geofizică în Arheologie. Investigații Non-Invazive în Așezări Cucuteni din România*; Universității Alexandru Ioan Cuza: Iași, Romania, 2019.
48. Gridan, S.; Urdea, P.; Hegyi, A. Castrul de la Ungra, jud. Brașov. Cercetări multidisciplinare. In *ArheoVest V2. Interdisciplinaritate în Arheologieși Istorie*; Forțiu, S., Ed.; JATE Press Kiadó: Szeged, Hungary, 2017; pp. 851–883.
49. Zăgrean, R.; Gridan, S.; Hegyi, A. *Castrul Roman de la Ungra (jud. Brașov)*; LIMES, Frontierele Imperiului Roman în România; Comisia Limes România: Bucharest, Romania, 2022; Volume 12, pp. 30–33.

Disclaimer/Publisher's Note: The statements, opinions and data contained in all publications are solely those of the individual author(s) and contributor(s) and not of MDPI and/or the editor(s). MDPI and/or the editor(s) disclaim responsibility for any injury to people or property resulting from any ideas, methods, instructions or products referred to in the content.